

SCIENTIFIC REPORTS



OPEN

Planktonic food web structure and trophic transfer efficiency along a productivity gradient in the tropical and subtropical Atlantic Ocean

Laia Armengol¹, Albert Calbet¹ , Gara Franchy¹, Adriana Rodríguez-Santos¹ & Santiago Hernández-León¹

Oligotrophic and productive areas of the ocean differ in plankton community composition and biomass transfer efficiency. Here, we describe the plankton community along a latitudinal transect in the tropical and subtropical Atlantic Ocean. *Prochlorococcus* dominated the autotrophic community at the surface and mixed layer of oligotrophic stations, replaced by phototrophic picoeukaryotes and *Synechococcus* in productive waters. Depth-integrated biomass of microzooplankton was higher than mesozooplankton at oligotrophic stations, showing similar biomasses in productive waters. Dinoflagellates dominated in oligotrophic waters but ciliates dominated upwelling regions. In oligotrophic areas, microzooplankton consumed ca. 80% of the production, but ca. 66% in upwelling zones. Differences in microzooplankton and phytoplankton communities explain microzooplankton diel feeding rhythms: higher grazing rates during daylight in oligotrophic areas and diffuse grazing patterns in productive waters. Oligotrophic areas were more efficient at recycling and using nutrients through phytoplankton, while the energy transfer efficiency from nutrients to mesozooplankton appeared more efficient in productive waters. Our results support the classic paradigm of a shorter food web, and more efficient energy transfer towards upper food web levels in productive regions, but a microbially dominated, and very efficient, food web in oligotrophic regions. Remarkably, both models of food web exist under very high microzooplankton herbivory.

On a global basis, microzooplankton (μZ) graze between 60 and 75% of primary production (PP) daily, whereas mesozooplankton (MZ) consume between 12 and 35%¹. Therefore, the combined impact of both groups account, on average, for ca. 3/4 of total PP². Given the important role of zooplankton in organic matter turnover, and to fully understand and model the ocean carbon cycle, the rate processes between producers and consumers and their biomass and community structure should be assessed at the ocean basin scale³. However, the trophic relationships between consumers and producers are highly variable and difficult to parameterize. For instance, authors have found bottom-up linkage, top-down control, or slight coupling between the different planktonic food web levels in different regions of the ocean⁴⁻⁷. This is to be expected, given the complexity and variability observed in systems of different trophic status⁸⁻¹⁰.

Oligotrophic food webs are substantially different to those from productive areas¹¹⁻¹³. However, general ecological rules should apply irrespective of the ecosystem under investigation (e.g., metabolic theory, Q_{10} concept, etc.). Thus, interconnecting the dynamics of diverse trophic areas is a challenge, and identification of the key processes influencing the dynamics of the marine food web has important implications in understanding the role of these organisms in the fate of carbon in the ocean. Numerous studies have addressed trophic relationships between planktonic organisms in the ocean, however, few studies have covered a wide spectrum of ecological scenarios¹⁴⁻¹⁷.

The warm and stratified subtropical gyres are oligotrophic areas covering approximately 40% of the planetary surface, and they are expanding 0.8–4.3%·y⁻¹¹⁸. Because of the large area they occupy, oligotrophic gyres have

¹Instituto de Oceanografía y Cambio Global (IOCAG), Universidad de Las Palmas de Gran Canaria (ULPGC), Unidad Asociada ULPGC-CSIC, Parque Científico Marino de Taliarte, Las Palmas de Gran Canaria, Spain. ²Institut de Ciències del Mar, CSIC, Passeig Marítim de la Barceloneta 37-49, 08003, Barcelona, Spain. Correspondence and requests for materials should be addressed to L.A. (email: laia.armengol@ulpgc.es)

an important influence on the contribution of PP and carbon export from the euphotic zone at the global scale¹⁸. Small cells predominate in these waters, and μ Z are more effective than MZ in preying upon phytoplankton, as a result of their similar size to phytoplankton, high growth rates, and high metabolism^{19–22}. Growth rates based on chlorophyll *a* (Chla) reported in the literature range from 0.1 to 2 d⁻¹ in these systems, probably due to the different phytoplankton responses to nutrient inputs and temperature^{23–27}. The major grazers, the μ Z, consume up to 70% of the PP in tropical and subtropical systems²⁸. Unlike oligotrophic areas where most likely dinoflagellates (Din) are the potential dominant microbial grazers, diatoms (Dia) dominate the autotrophic community in more productive systems²⁹. Even in these rich waters, μ Z are the major grazers, consuming ca. 60% of the PP^{2,30}. Additionally, MZ have been reported as important consumers of μ Z in oligotrophic environments and, with less impact, in upwelling systems³¹. Therefore, the relationship between these two important groups of organisms (i.e. μ Z and MZ) influences the energy and carbon flow throughout the food web²⁹.

In this study we investigated a wide range of different scenarios in the tropical and subtropical regions, from oligotrophic to productive areas. We aimed to understand the trophic relationships from pico- to MZ at the basin scale from 13°S to 25°N in the Atlantic Ocean. Physico-chemical (temperature, salinity, oxygen, and inorganic nutrients) and biological variables (μ Z and MZ biomass and μ Z grazing) were studied in environments as different as the subtropical gyre and the African upwelling system.

Results

Hydrological structure. We observed a sharp temperature and density gradient along the transect, as expected (Fig. 1). A convergence of the South Equatorial Counter Current (SECC; Reid³²) showed a deeper thermocline and high salinity (Stations 1 to 3), while the Equatorial Divergence within the South Equatorial Current (SEC) promoted a shallower thermocline and a decrease in dissolved oxygen concentration (Station 4) (Fig. 1). The Intertropical Convergence Zone (ITCZ) showed the slightly deepest thermocline as well as high oxygen concentration levels (between Stations 5 and 6). At Station 8, the North Equatorial Current (NEC) lowered the temperature northward of 10°N and produced an oxygen minimum zone (OMZ). Station 9 showed typical features of the Guinea Dome, characterized by anticyclonic thermal and saline structure. The upwelling off Cape Blanc produced cold temperatures and less stratified waters (Stations 10 and 11), while the Canary Current presented waters with high salinity and oxygen concentration (Station 12, Fig. 1).

Nutrient distribution. Inorganic nutrient concentrations were higher below the thermocline throughout the transect, as expected (Fig. 2). The highest values for nitrite were found at the Equatorial Divergence, at the mid-ocean upwelling below 50 m depth, at Guinea Dome, and on the surface at the Cape Blanc upwelling (Fig. 2a). Nitrates, phosphates, and silicates showed a core around 50 m depth in the Equatorial Divergence, while from the mid-ocean upwelling (Station 6) to the Cape Blanc upwelling nutrients concentration increased in the mixed layer. The Guinea Dome made an exception because nutrients decreased in the upper layers at this site (Fig. 2b–d). Ammonium levels were slightly higher near the thermocline but showing an important increase (>2 μ mol L⁻¹) near the Guinea Dome (Stations 8 and 9, Fig. 2e).

Phytoplankton community. Along the transect, the Chla maximum (CM) followed the base of the thermocline (Fig. 3), which was deeper in the warmest and oligotrophic areas (Stations 1–3), and shallower in the coldest and upwelling-influenced areas (Stations 10 and 11). The CM showed the highest values at the mid-ocean equatorial upwelling and Cape Blanc upwelling. Conversely, the lowest Chla values were observed at the surface and at the mixed layer (ML) in the oligotrophic area (Figs 3 and 4a). The Kendall Rank correlation test showed a positive correlation between Chla and nutrient concentration ($\tau = 0.69$, $p < 0.001$ for $\text{NO}_3 + \text{NO}_2$; and $\tau = 0.57$, $p < 0.001$ for phosphates). Physical factors, such as temperature and nutrient concentration, as well as MZ biomass explained 85.2% of the variance in the distribution of Chla (PCA and GAM tests, Table 1). The signature of the Guinea Dome and Northwest African upwelling were also conspicuous on the satellite data, showing rather high values of PP (Fig. 5).

The biomass of phototrophic picoplankton, based on cytometry data, increased from oligotrophic to upwelling regions (Fig. 4), with a further decrease at the Cape Blanc upwelling (Station 11), where Chla showed maximum concentrations (Fig. 3). *Prochlorococcus* (*Proch*) dominated at the surface and ML at the most oligotrophic and warmest stations and was replaced by *Synechococcus* (*Syn*) in more productive waters. Picoeukaryotes (PE) dominated the autotrophic community at stations with low temperatures and high nutrient availability, such as in the Guinea Dome and Cape Blanc upwelling zone, as well as at the CM throughout all stations (Kendall Rank correlation test $\tau = 0.61$, $p < 0.001$ for $\text{NO}_3 + \text{NO}_2$) (Fig. 6). 81% of *Proch* and 64.1% of PE biomass variability was explained by temperature, nutrients, μ Z, and MZ, whereas *Syn* distribution was determined by temperature (75.2%), μ Z, and MZ (PCA and GAM tests, Table 1).

Micro- and mesozooplankton community. The oligotrophic stations and mid-ocean upwelling showed the highest μ Z biomass (mean 20.61 ± 3.49 SE mgC m⁻³), and its importance decreased along the transect (Fig. 6a–c) as temperatures fell. Chla, PE, *Syn*, and MZ explained 85% of μ Z biomass variability (PCA and GAM tests, Table 1). Din biomass dominated the microzooplankton in the warmest and stratified waters, comprising 60–80% of total μ Z biomass. From the mid-ocean upwelling, Din dominance became irregular with decreasing abundance and an increasing abundance of the naked ciliates (*Cil*) (Fig. 6b). This change in micro-grazer dominance was especially evident in upwelling stations where temperatures decreased sharply. Tintinnids contributed <5% of the total μ Z biomass at all stations (Fig. 6b).

MZ biomass increased along the transect (Fig. 6c) with temperature decrease, showing the lowest MZ biomass in the oligotrophic region (mean 4.89 ± 1.64 SE mgC m⁻³) (Fig. 6c). In size terms, the organisms of the MZ with

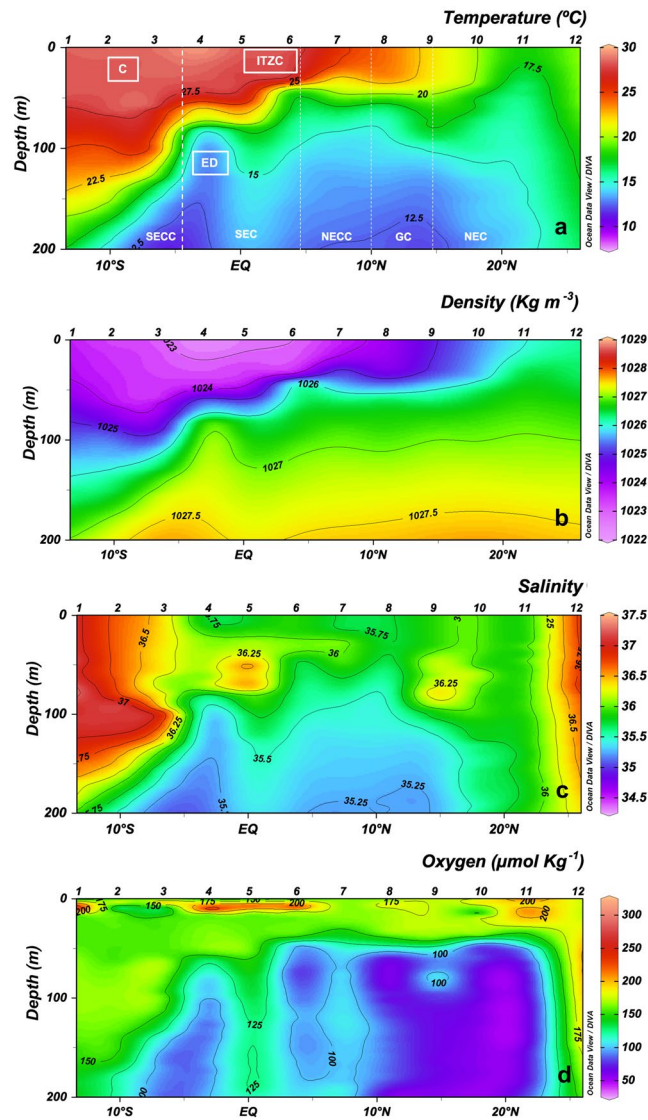


Figure 1. Vertical section (0–200 m) of (a) temperature ($^{\circ}\text{C}$), water currents (South Equatorial Counter Current (SECC), South Equatorial Current (SEC), North Equatorial Counter Current (NECC), Guinea Dome (GD), North Equatorial Current (NEC)) and physical processes (Convergence (C), Equatorial divergence (ED), Intertropical Convergence Zone (ITCZ)); (b) density (Kg m^{-3}); (c) salinity; and (d) dissolved oxygen ($\mu\text{mol Kg}^{-1}$) along transect in the Atlantic basin, based on CTD data. Biogeochemical areas are indicated at the top of panels.

a size $>1000\mu\text{m}$ dominated the MZ community at all stations, although the biomass of organisms between 500 and $1000\mu\text{m}$ increased at Stations 8 and 9.

Microzooplankton grazing. Potential phytoplankton growth rates based on Chla (μ_{Chla}) in the ML were higher at the oligotrophic stations within the SECC and Equatorial Divergence than at other oligotrophic stations (Fig. 7a; Table 2). However, the growth rates of the different groups of autotrophs differed from those based on Chla (Fig. 7, Table 2) showing significant differences between oligotrophic and productive areas ($p < 0.001$; Wilcoxon-Mann-Whitney test). PE and *Syn* potential growth rates (μ_{PE} , μ_{Syn}) showed slightly higher values at the surface and ML in productive areas (mean $0.52 \pm 0.08 \text{ SE d}^{-1}$ and $0.65 \pm 0.14 \text{ SE d}^{-1}$, for PE and *Syn* respectively), and the lowest rates (mean $0.23 \pm 0.07 \text{ SE d}^{-1}$ for PE and $0.36 \pm 0.07 \text{ SE d}^{-1}$ for *Syn*) at oligotrophic stations ($p < 0.001$; Wilcoxon-Mann-Whitney test for PE and t-test for *Syn*) (Fig. 7b,c). Potential growth rates for *Proch* (μ_{Pro}) were lower than for other picoplankton organisms at all stations except Station 3 (Fig. 7d). At CM, potential growth rates for autotrophic picoplankton and Chla showed non-significant differences between oligotrophic and productive areas (t-test for μ_{Chla} and μ_{Syn} ; Wilcoxon-Mann-Whitney test for μ_{PE} and μ_{Pro} ; Fig. 7, Table 2).

At the surface and ML, μZ grazing rates on phytoplankton based on Chla (g_{Chla}) showed the highest rates at SECC and Equatorial Divergence (Stations from 1 to 4) (Fig. 8A; Table 2). Also, at the surface and ML, grazing rates on PE (g_{PE}) and *Syn* (g_{Syn}) were significantly lower at oligotrophic stations ($0.19 \pm 0.05 \text{ SE}$ for PE and 0.28

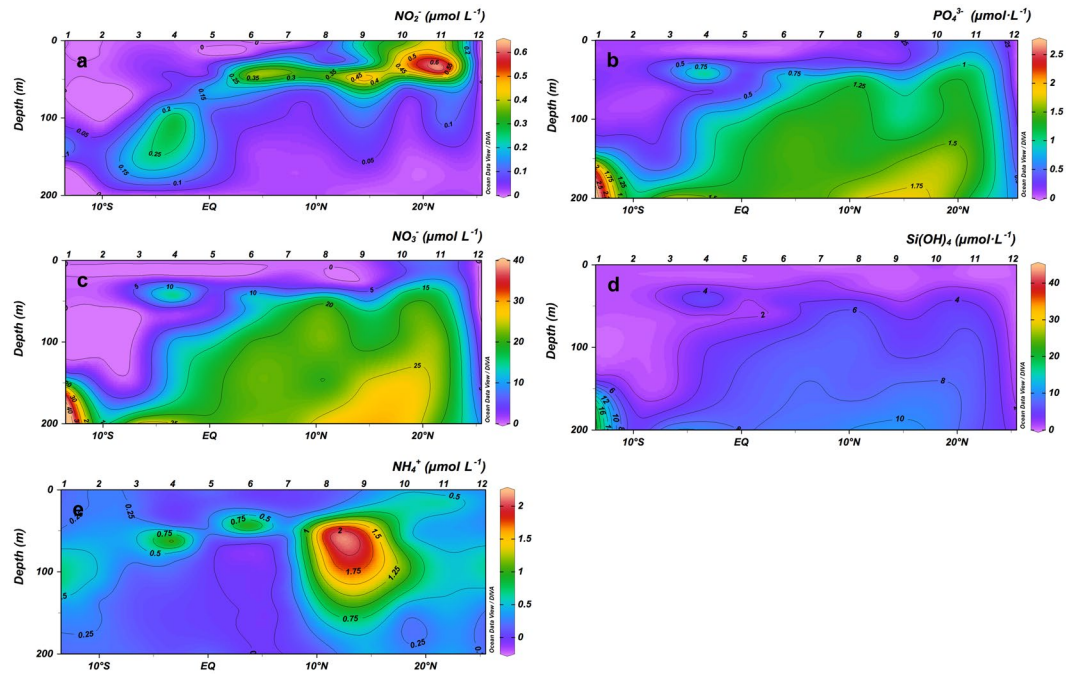


Figure 2. Vertical section (0–200 m) of (a) nitrites, (b) phosphates, (c) nitrates, (d) silicates and (e) ammonia ($\mu\text{mol L}^{-1}$).

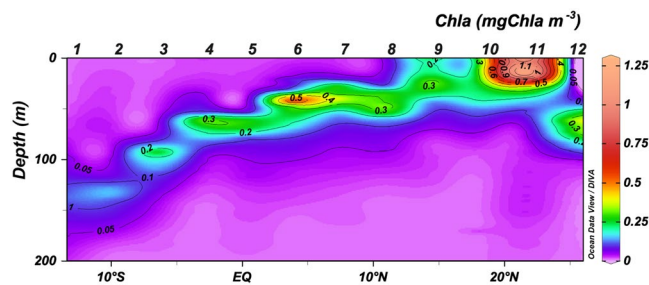


Figure 3. Vertical section (0–200 m) of Chlorophyll *a* (mgChla m^{-3}).

± 0.05 SE for *Syn*) than at productive stations (0.38 ± 0.06 SE for PE and 0.41 ± 0.09 SE for *Syn*) ($p < 0.001$ Wilcoxon-Mann-Whitney for PE; and $p < 0.01$ t-test for *Syn*) (Fig. 9b,c; Table 2). The μZ grazing rates on *Proch* (g_{Proch}) were higher at the surface and ML at stations with a shallower thermocline (Stations 5 to 8; Fig. 8d; Table 2). At CM, μZ grazing rates of Chla, PE, *Syn* and *Proch* showed a non-significant difference between oligotrophic and productive regions (Wilcoxon-Mann-Whitney test for Chla, *Syn* and *Proch*; t-test for PE) (Fig. 8, Table 2). Overall, μZ grazing rates for all organisms were lower at the CM than in the upper layers (Fig. 8, Table 2).

The ratio of grazing rates to phytoplankton growth (g/μ) provided an estimate of the proportion of the potential PP consumed by microbial grazers (%PP). Based on Chla the %PP_{Chla} showed non-significant differences (t-test) from oligotrophic to upwelling areas at the surface and ML (Fig. 9a). In the same water column range, the impact upon PE (%PP_{PE}) and *Syn* (%PP_{Syn}) were higher in the oligotrophic areas (134.75 ± 25.03 SE for PE; 108.01 ± 19.04 SE for *Syn*) than in the upwellings (79.15 ± 7.28 SE for PE; 69.01 ± 8.63 SE for *Syn*) ($p < 0.05$ for PE and $p < 0.01$ for *Syn* Wilcoxon-Mann-Whitney test), while the impact of grazers on *Proch* (%PP_{Proch}) increased at the surface with more shallow thermoclines, except in the equatorial regions (Wilcoxon-Mann-Whitney test) (Fig. 9b–d).

Diel growth and grazing rates. No clear pattern of diel growth and grazing were observed based on total Chla (Fig. 10a). However, a more detailed study of different groups of plankton showed different daily patterns. PE and *Syn* displayed a clear rhythm in both growth and grazing, with higher rates during the day, while this pattern vanished in upwelling waters (Fig. 10b,c). *Proch* showed higher growth and grazing rates during night in the most oligotrophic and stratified areas (Stations 1 and 2), but the rhythm was the opposite in the Equatorial Divergence (Stations 4 and 5, Fig. 10d, Table 3).

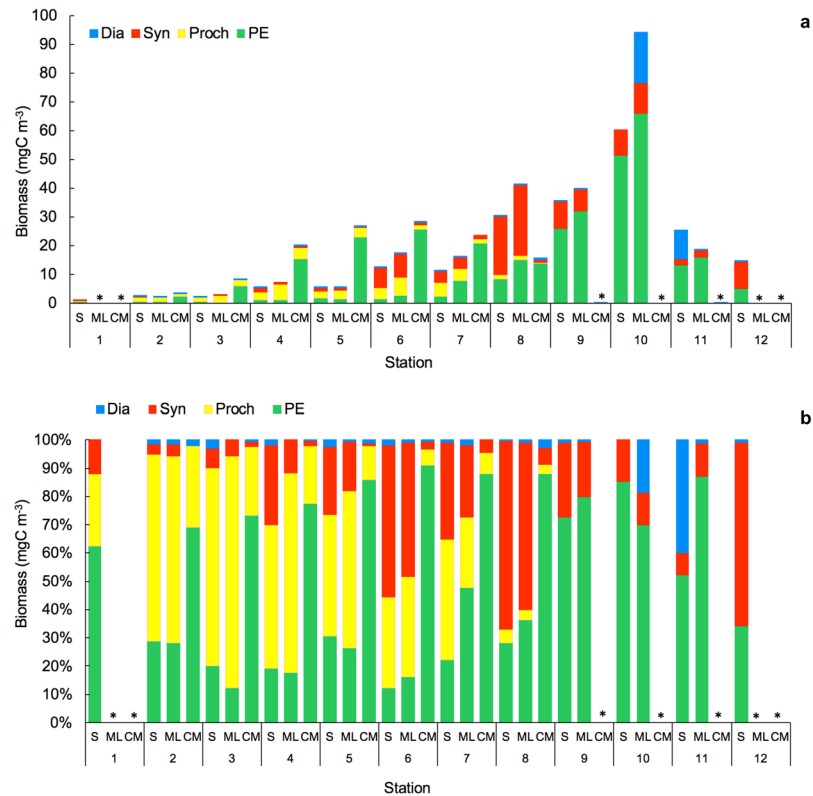


Figure 4. (a) Proportion of biomass (%) and (b) Biomass (mgC m^{-3}) of Cyanobacteria (*Synechococcus*, Syn; *Prochlorococcus*, Proch; and picoeukaryotes, PE) at the surface layer (5 m depth, S), mixed layer (between 20–30 m depth, ML) and chlorophyll *a* maximum (CM). *No data available.

Trophic transfer efficiency. The ratio between the biomass of upper and lower trophic levels can be used as a proxy measure of the trophic transfer efficiency within the food web. Thus the ratio of Chla:($\text{NO}_2 + \text{NO}_3$) showed that each μM of N sustained, on average, $22.9 \mu\text{g C}$ of phytoplankton ($\pm 16.86 \text{ SE}$) in oligotrophic regions, and $2.6 \mu\text{g C}$ of phytoplankton ($\pm 0.74 \text{ SE}$) in productive regions. The ratio between biomass of $\mu\text{Z}:(\text{NO}_2 + \text{NO}_3)$ showed that each μmol of N supported $27.9 \mu\text{g C}$ of μZ ($\pm 12.98 \text{ SE}$) in oligotrophic zones, whereas for productive areas this decreased to $2.9 (\pm 0.68 \text{ SE}) \mu\text{g C}$ of μZ . For MZ, the ratio between their biomass and $\text{NO}_2 + \text{NO}_3$ resulted in lower values than for μZ at oligotrophic stations (mean $5.8 \mu\text{g}$ of MZ $\pm 1.26 \text{ SE}$), while at productive stations values were higher than for μZ (mean $14.2 \mu\text{gC}$ of MZ $\pm 7.83 \text{ SE}$). The carbon transferred from phytoplankton to μZ (μZ biomass:phytoplankton biomass) averaged $3.9 \pm 0.68 \text{ SE}$ at oligotrophic stations, and decreased to $0.70 \pm 0.39 \text{ SE}$ at productive stations. Using the same quotient for MZ, in oligotrophic areas the ratios were slightly lower (mean $0.92 \pm 0.44 \text{ SE}$) than in productive areas (mean $1.28 \pm 0.33 \text{ SE}$). MZ biomass supported by μZ biomass averaged $0.15 \pm 0.03 \text{ SE}$ in oligotrophic areas, and $1.44 \pm 0.33 \text{ SE}$ in the upwelling region.

Discussion

Major differences between oligotrophic and productive zones: from organismal abundances to trophic transfer efficiencies.

The main finding of this study was the close relationship between the distribution and trophic relationships of the planktonic organisms with the physical variables characterizing each geographical region. However, for the sake of simplicity and in spite of the distinctive characteristics of the areas surveyed, we will focus in this section on the oligotrophic and more productive zones, merging the different regions studied into these two categories. In this regard, at the very base of the marine food web, we found that prokaryotes dominated the autotrophic community in oligotrophic areas³³, most likely because they are more efficient than protists at assimilating nutrients at low concentrations due to their higher cell surface-to-volume ratio³⁴. In particular, *Proch* was more abundant in the oligotrophic and warmest waters, whereas *Syn* and PE showed higher biomass in colder and nutrient richer waters (Fig. 4). Differences in their cell structure and physiology may explain this zonation, already reported in other studies^{35–37}. *Proch* and *Syn* differ in size and light-harvesting antenna systems and the former is unable to use nitrates, whereas *Syn* uses them as a main source of N (for a review, see^{38–41}). Moreover, *Proch* takes up phosphate in nutrient-depleted zones as a result of phosphate-specific acquisition genes, which gives these organisms an advantage in oligotrophic areas^{42,43}. These features explained their dominance at the surface and ML in the South Atlantic gyre and Equatorial Divergence. Higher PE biomass occurred in areas with relatively high concentration of nutrients, as in the CM and upwelling regions, in accordance with observations by Tarran⁴⁴. Also, as expected, *Dia* made a large contribution to the biomass at the

Model	PCA (variance, %)	GAM					
		Residual Df	F or t	Deviance explained	R-sq (adj)	GCV	Scale est.
<i>Chlorophyll a</i> Terms:	85.2%			71.2%	0.68	75.31	64.55
+Temperature			-3.19**				
+NO ₃			1.6				
+Mesozooplankton			2.3**				
<i>PE</i> Terms:	64.1%			99.3%	0.92	39.57	20.93
Temperature		7.65	22.74***				
NO ₃		2.64	9.99**				
Mesozooplankton		8.98	16.8***				
<i>Synechococcus</i> Terms:	75.2%			95.8%	0.9	8.05	3.72
NO ₃		2.46	37.64***				
Dinoflagellates		6.24	3.23*				
Mesozooplankton		5.79	19.89***				
<i>Prochlorococcus</i> Terms:	81%			81.5%	0.68	1.83	1.00
Temperature		7.52	3.96**				
NO ₃		3.08	1.19				
Microzooplankton		1.00	2.01				
Microzooplankton Terms:	85%			70.6%	0.57	204.4	144.56
Temperature		2.06	9.37**				
Chlorophyll <i>a</i>		3.84	4.68**				
Mesozooplankton		1.00	0.003				
Mesozooplankton Terms:	85.2%			85.4%	0.74	53.09	29.45
Temperature		3.02	4.39*				
Chlorophyll <i>a</i>		2.50	6.98**				
Microzooplankton		6.74	1.70				

Table 1. Principal Component Analysis (PCA) and Generalized Additive Model (GAM) for groups of organisms using biological and physical variables as effects; n = 28. Residual Degrees of Freedom (Df). +t-value for linear adjust and F-value for smooth adjust. Significance level: *p < 0.1; **p < 0.01; ***p < 0.001.

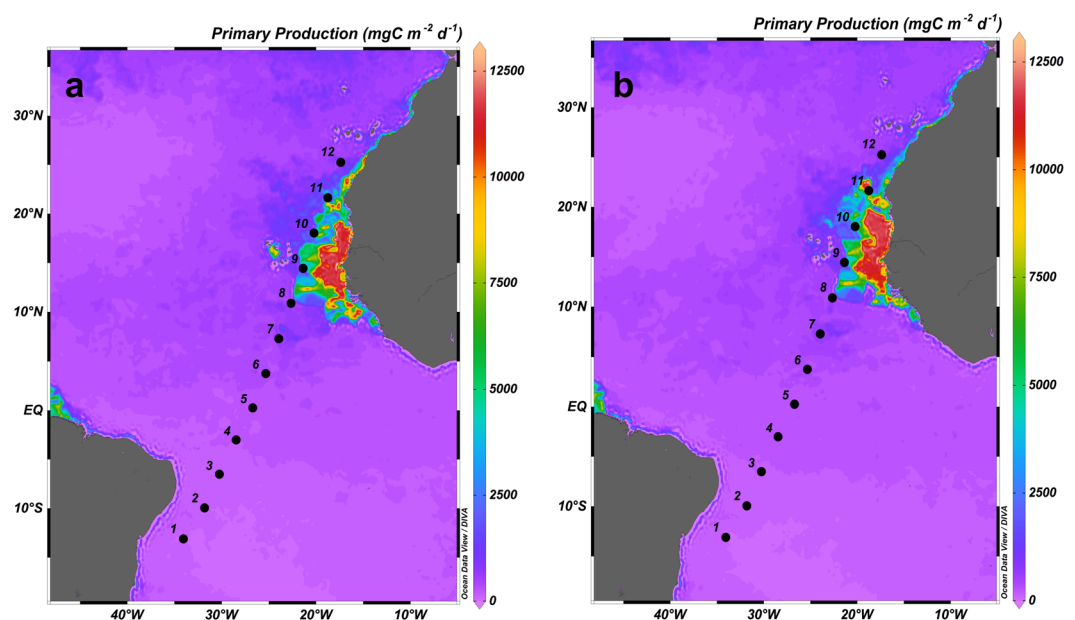


Figure 5. Surface maps of Primary Production ($\text{mgC m}^{-2} \text{d}^{-1}$) from satellite data during 15–22 April (a) and 23–30 April (b).

upwelling station although they did not dominate the community, as also observed by Marañón⁴⁵. The strong relationship between $\text{NO}_2 + \text{NO}_3$ and primary producers is mainly because NO_3 is the most commonly consumed and reduced form of nitrogen for building organic molecules⁴⁶ and NO_2 plays an intermediary role in the global cycles of nitrogen and carbon and in microbial metabolism. The biotic responses to nutrient concentration can

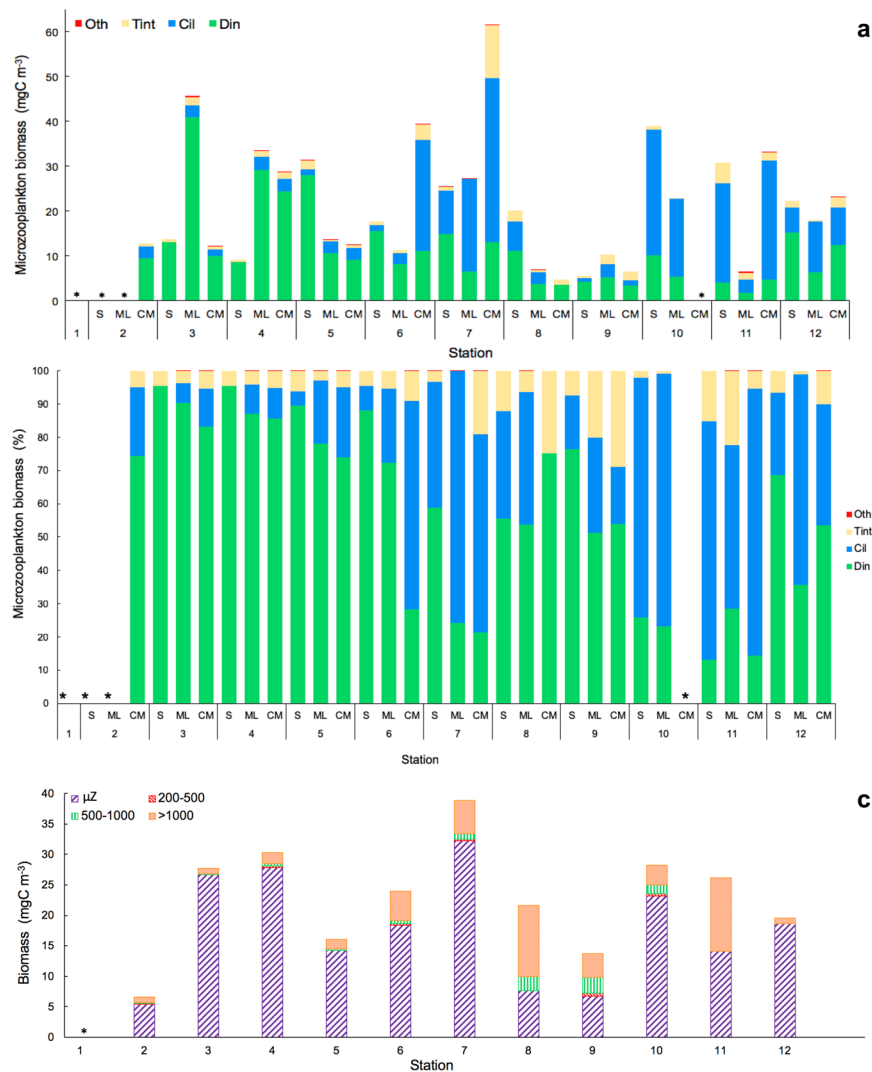


Figure 6. Biomass of dinoflagellates (Din), ciliates (Cil), tintinnids (Tint), and others microzooplankton groups (Oth) (a) in mgC m^{-3} and (b) in %; (c) Integrated biomass (mgC m^{-3}) in the water column of microzooplankton (μZ) and different mesozooplankton size-fraction: 200–500 μm (200–500), 500–1000 μm (500–1000) and >1000 μm (>1000). *No data available.

be direct, such as shifts in phytoplankton community composition, or indirect, such as shifts in grazer community composition^{47,48}. It is well known, however, that the biomass and distribution of phytoplankton do not solely depend on nutrient availability or temperature; grazing is also an important factor shaping autotrophic communities^{49,50}. Our results, similar to those of Calbet and Landry³⁰, show that at the surface and ML of the oligotrophic ocean μZ consumed approximately 78% of the PP, whereas in upwelling areas consumption was slightly lower (~66%, Fig. 9). The μZ of oligotrophic regions showed low efficiency in consuming *Proch* (Figs 9d and 10d)^{51,52}; however, μZ grazing rates on *Proch* rose at the ITCZ and mid-ocean upwelling stations, coinciding with an increase in PE (Fig. 6b), which have been documented to be efficient mixotrophs^{43,53,54}. Therefore, high grazing rates on *Proch* in those areas may be due to a cascade effect where MZ (which increased their biomass) consume μZ (decreasing their biomass) (Fig. 6a), releasing PE from grazing pressure and increasing their biomass, which in turn increases *Proch* consumption ($\tau = -0.27$, $p < 0.05$; Kendall Rank correlation test between biomass of *Proch* and PE). *Syn* consumption was similar throughout the basin, indicating that Din, which dominated the μZ community in oligotrophic regions (Fig. 6c), and *Cil* consume them at similar rates (e.g. refs^{55–57}). In warm oligotrophic regions, where prey are smaller and less numerous, Din dominated the microplankton community (Fig. 6c), as opposed to upwelling areas, where the μZ was dominated by *Cil*. It is known that copepods show a low preference for predation upon Din^{58,59}, and show preference for *Cil* (e.g.⁶⁰). This copepod prey selectivity could explain the decrease in μZ biomass compared to MZ in the upwelling areas. Furthermore, higher predation levels on μZ released PE and *Syn* from grazing pressure, facilitating a rise in their biomass (e.g.⁶⁰). A fingerprint of this cascade effect was the positive correlation between MZ biomass and picoautotroph cells.

Overall, in the oligotrophic Atlantic, each μM of N supported far more phytoplankton than in the Northwest African upwelling. This result is not surprising because oligotrophic food webs are known to recycle nutrients

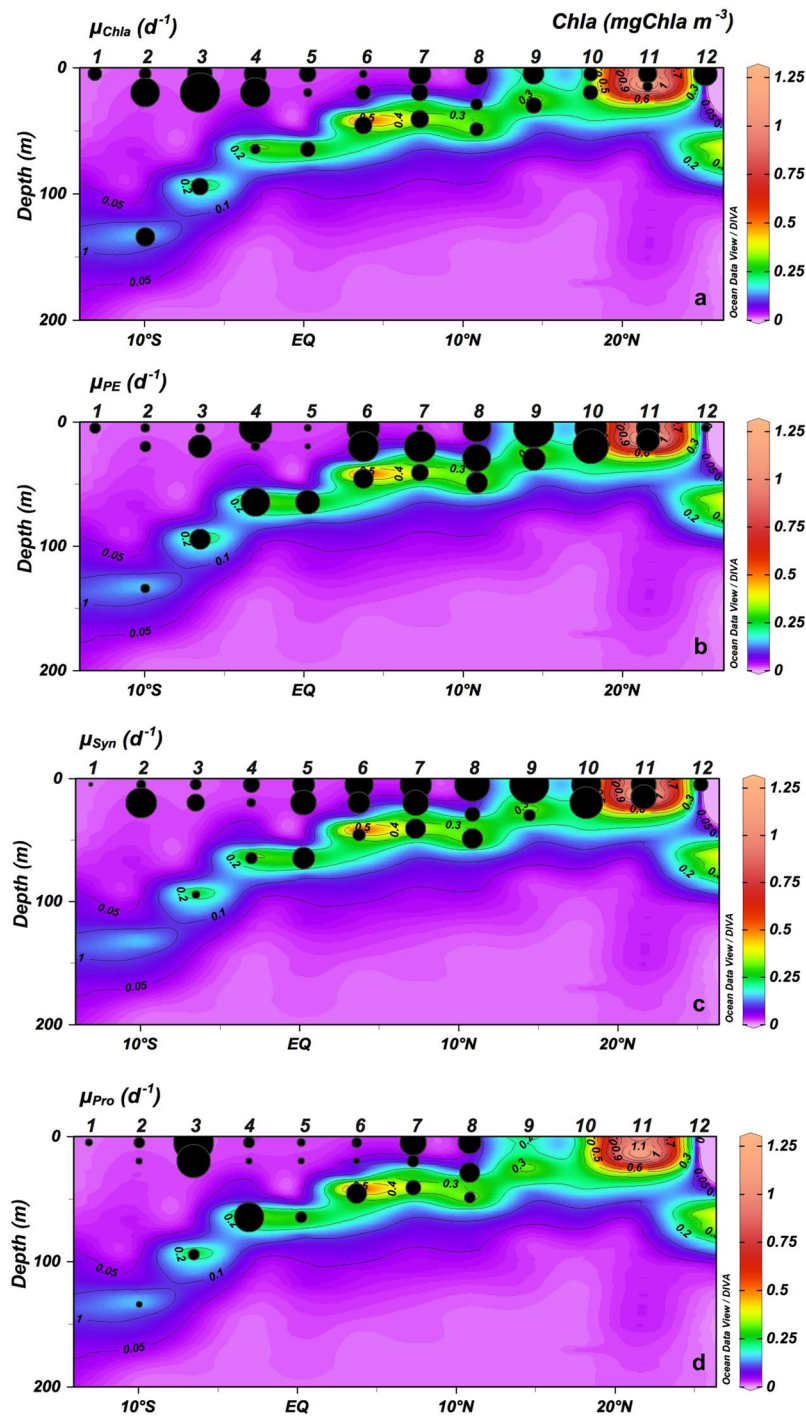


Figure 7. Vertical section (0–200 m) of Chlorophyll *a* (mgChla m^{-3}) and potential growth rates (μ , d^{-1}) for (a) Chlorophyll *a* (μ_{Chla}), (b) picoeukaryotes (μ_{PE}), (c) *Synechococcus* (μ_{Syn}) and (d) *Prochlorococcus* (μ_{Pro}).

more efficiently, also allowing for a proportionally higher biomass of μZ than very productive ones^{61–63}. The proportional increase in μZ biomass at the oligotrophic stations did not imply an increase in biomass transfer upwards to MZ, since in oligotrophic environments the carbon of μZ that supported MZ is smaller than in the upwelling areas. These results demonstrate the bottom-up control of μZ in oligotrophic areas, and suggest a closer link between MZ and μZ in upwelling regions. Moreover, each μM of N supports more MZ at productive sites, manifesting the higher linear transfer efficiency of energy in productive ecosystems than in oligotrophic ecosystems^{62,63}. Therefore, our results regarding food web trophic efficiency back up the paradigm of much more efficient recycling in oligotrophic conditions, but with an overall lower linear energy transfer towards higher trophic levels. In other words, our data fully support the existence of a strong microbial loop in oligotrophic areas and a more classic food chain in more productive regions (e.g. refs^{64–66}). Interestingly, these findings do not contradict

Station	Depth (m)	Growth (d^{-1})				Grazing (d^{-1})			
		μ_{Chla}	μ_{PE}	μ_{Syn}	μ_{Proch}	g_{Chla}	g_{PE}	g_{Syn}	g_{Proch}
1	5	0.155 ± 0.00	0.073 ± 0.03	0.013 ± 0.01	0.031 ± 0.000	0.177 ± 0.034	0.186 ± 0.014	0.298 ± 0.123	0.114 ± 0.043
2	5	0.119 ± 0.048	0.047 ± 0.027	0.073 ± 0.006	0.071 ± 0.008	0.098 ± 0.005	0.071 ± 0.024	0.265 ± 0.02	0.001 ± 0.024
	20	0.666 ± 0.025	0.069 ± 0.03	0.783 ± 0.039	0.001	0.682 ± 0.009	0.086 ± 0.005	0.705 ± 0.027	0.055 ± 0.01
	135 (CM)	0.285 ± 0.041	0.048 ± 0.011	0.001	0.024 ± 0.013	0.179 ± 0.029	0.134 ± 0.008	0	0.047 ± 0.004
3	5	0.502 ± 0.015	0.05 ± 0.031	0.106 ± 0.023	0.952 ± 0.047	0.421 ± 0.013	0.046 ± 0.022	0.18 ± 0.022	0.83 ± 0.031
	20	1.26 ± 0.013	0.318 ± 0.052	0.259 ± 0.059	0.673 ± 0.065	0.769 ± 0.007	0.325 ± 0.006	0.247 ± 0.019	0.718 ± 0.027
	95 (CM)	0.229 ± 0.021	0.252 ± 0.055	0.05 ± 0.017	0.073 ± 0.01	0.167 ± 0.034	0.197 ± 0.019	0.12 ± 0.007	0.057 ± 0.014
4	5	0.400 ± 0.021	0.642 ± 0.104	0.221 ± 0.048	0.074 ± 0.017	0.023 ± 0.051	0.547 ± 0.033	0.249 ± 0.016	0.148 ± 0.022
	20	0.706 ± 0.077	0.045 ± 0.018	0.064 ± 0.005	0.001	0.647 ± 0.021	0.071 ± 0.045	0.081 ± 0.01	0
	65 (CM)	0.077 ± 0.008	0.495 ± 0.05	0.113 ± 0.024	0.527 ± 0.027	0.114 ± 0.027	0.416 ± 0.039	0.092 ± 0.01	0.515 ± 0.01
5	5	0.226 ± 0.048	0.032 ± 0.007	0.396 ± 0.099	0.039 ± 0.023	0	0.058 ± 0.019	0.322 ± 0.041	0.093 ± 0.022
	20	0.061 ± 0.010	0.019 ± 0.009	0.535 ± 0.037	0.001	0.095 ± 0.003	0.062 ± 0.014	0.483 ± 0.012	0.582 ± 0.085
	65 (CM)	0.182 ± 0.018	0.341 ± 0.04	0.397 ± 0.043	0.077 ± 0.012	0.148 ± 0.009	0.303 ± 0.01	0.345 ± 0.027	0.077 ± 0.011
6	5	0.051 ± 0.024	0.642 ± 0.007	0.653 ± 0.067	0.063 ± 0.022	0.081 ± 0.006	0.283 ± 0.009	0.331 ± 0.095	0.093 ± 0.007
	20	0.187 ± 0.024	0.568 ± 0.043	0.408 ± 0.029	0.001	0.161 ± 0.020	0.232 ± 0.027	0.056 ± 0.36	0.544 ± 0.037
	46 (CM)	0.241 ± 0.018	0.225 ± 0.018	0.129 ± 0.008	0.237 ± 0.014	0.205 ± 0.005	0.022 ± 0.023	0.113 ± 0.007	0.249 ± 0.012
7	5	0.408 ± 0.036	0.027 ± 0.014	0.81 ± 0.093	0.409 ± 0.115	0.162 ± 0.015	0	0.183 ± 0.038	0.392 ± 0.011
	20	0.228 ± 0.056	0.593 ± 0.044	0.549 ± 0.025	0.09 ± 0.023	0.153 ± 0.006	0.538 ± 0.014	0.449 ± 0.032	0.593 ± 0.025
	41 (CM)	0.256 ± 0.011	0.169 ± 0.034	0.334 ± 0.049	0.132 ± 0.009	0.181 ± 0.020	0.221 ± 0.015	0.306 ± 0.024	0.178 ± 0.007
8	5	0.426 ± 0.038	0.475 ± 0.079	1.016 ± 0.111	0.24 ± 0.027	0.316 ± 0.017	0.239 ± 0.014	0.658 ± 0.063	0.309 ± 0.011
	29	0.112 ± 0.026	0.47 ± 0.015	0.181 ± 0.047	0.073 ± 0.016	0.144 ± 0.026	0.224 ± 0.075	0.134 ± 0.019	0.493 ± 0.013
	49 (CM)	0.142 ± 0.026	0.265 ± 0.022	0.336 ± 0.029	0.003 ± 0.001	0 ± 0.037	0.294 ± 0.004	0.242 ± 0.025	0.096 ± 0.013
9	5	0.356 ± 0.052	0.939 ± 0.007	1.238 ± 0.037		0.082 ± 0.067	0.621 ± 0.032	0.56 ± 0.022	
	30 (CM)	0.198 ± 0.016	0.313 ± 0.049	0.11 ± 0.031		0.209 ± 0.010	0.29 ± 0.01	0.098 ± 0.012	
10	5	0.159 ± 0.006	0.609 ± 0.023	0.711 ± 0.066		0.040 ± 0.011	0.398 ± 0.036	0.426 ± 0.041	
	20	0.170 ± 0.013	0.737 ± 0.054	0.868 ± 0.064		0.110 ± 0.021	0.68 ± 0.026	0.725 ± 0.011	
11	5	0.273 ± 0.008	0.329 ± 0.047	0.523 ± 0.016		0.250 ± 0.007	0.298 ± 0.044	0.182 ± 0.021	
	15 (CM)	0.076 ± 0.026	0.315 ± 0.047	0.516 ± 0.013		0	0.311 ± 0.005	0.497 ± 0.01	
12	5	0.442 ± 0.080	0.043 ± 0.009	0.173 ± 0.025		0	0.079 ± 0.019	0.115 ± 0.029	

Table 2. Phytoplankton growth (μ) and microzooplankton grazing (g) rates (d^{-1}) for total chlorophyll a (Chla), picoeukaryotes (PE), *Synechococcus* (Syn) and *Prochlorococcus* (Proch) from seawater dilution experiments at surface (5 m), mixed layer (20 m) and chlorophyll maximum (CM). Negative growth and grazing rates were converted to 0.001 and 0, respectively. Note *Proch* were not present at stations 9 to 12. Values (mean \pm SE).

the fact that μZ grazing can be very high in productive regions as well, as occurred here, and actually merge the settled paradigms of food web structure (microbial loop for oligotrophic areas and classic food chain for upwellings) with the predominance of the μZ grazing over the MZ in marine ecosystems^{2,30}.

Vertical zonation. The CM in oligotrophic areas is formed as a result of the photoacclimation of the cells and/or an increase in phytoplankton growth due to nutrient diffusion through the thermocline. The biomass-specific grazing on Chla and upon each autotrophic group was lower in the CM than at the surface and ML (Fig. 8). As hypothesized by Landry *et al.*⁶⁷, low grazing rates in areas with high availability of resource, as in the CM, could be a consequence of low concentrations of μZ . Moreover, previous studies found lower growth rates in this environment than in the ML, suggesting a low turnover of the phytoplankton community^{25,68,69}, or as in our case, may be the result of an overestimation of phytoplankton production due to our assessment of the potential growth of autotrophic organisms. Worden and Binder⁷⁰ found non-significant differences between growth rates with and without nutrient addition treatments in oligotrophic areas, indicating that growth rates respond to nutrient enrichment at time scales greater than 24 hours or that there may be a lack of nutrient limitation due to fast recycling. If this were the case in our study we should consider the estimated potential growth rates at oligotrophic stations similar to the real rates. Conversely, growth rates based on Chla (Fig. 7a) in surface layers at the productive stations (the mid-ocean upwelling, Guinea Dome and Northwest African upwelling) were similar to those obtained by Marañón *et al.*²⁵ where, as in this study, the nitracline occurred at a similar depth.

Diel cycles of microzooplankton grazing. Previous studies showed that daily variations in phytoplankton in oligotrophic areas were more important than seasonal or annual changes^{71–73}. Certainly cloud cover, sinking, advection, and turbulence transporting cells between darkness and full sunlight⁷⁴ modify the intensity of light experienced by cells in the ocean and may have important consequences on phytoplankton growth. In general, light controls cell cycles in many phytoplankters either directly or by adjusting the biological clock^{75,76}. For picoplankton, cell division begins near dusk, with *Syn* starting the process, followed by *Proch*, and finally PE^{77,78}. Conversely, cell-biomass increases during daylight hours^{78–80}, as we observed at the oligotrophic stations (Fig. 10).

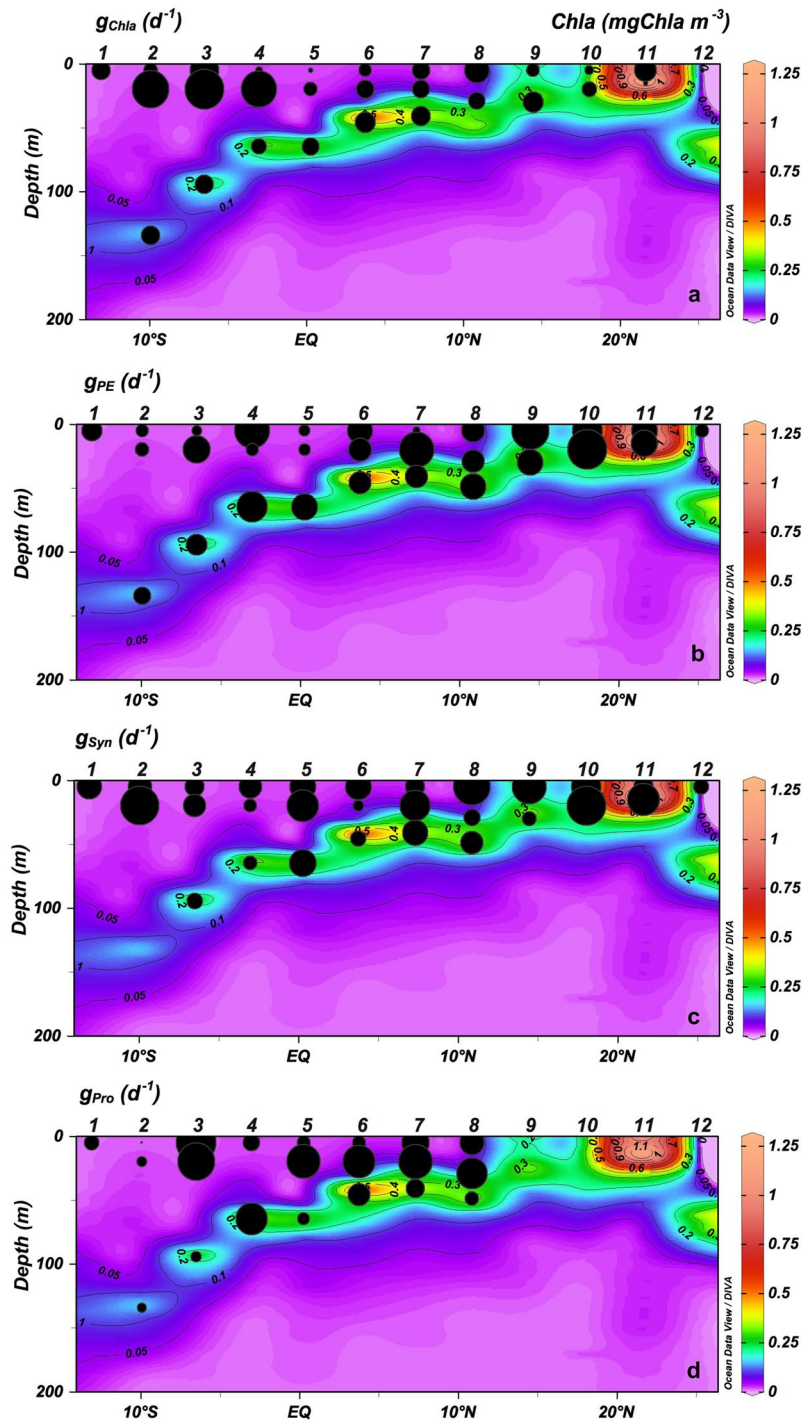


Figure 8. Vertical section (0–200 m) of Chlorophyll *a* (mgChla m^{-3}) and microzooplankton grazing rates (g d^{-1}) for (a) Chlorophyll *a* (g_{Chla}), (b) picoeukaryotes (g_{PE}), (c) *Synechococcus* (g_{Syn}) and (d) *Prochlorococcus* (g_{Pro}).

Diel cycles of growth have also been identified for μZ species, such as *Gymnodinium* sp.⁸¹ or *Coxiella* sp.⁸², which showed higher growth rates during daylight, with a few exceptions⁸³. Likewise, specific protozoan grazing activity seems to occur mostly during the day^{82,84–87}. The reasons for this rhythm could be endogenous circadian cycles, light-aided digestion, or diel variations in phytoplankton stoichiometry^{82,83,85–87}. Recently, Arias *et al.*⁸⁵ have suggested that the diel rhythms in μZ were inverse to those of their consumers in order to avoid being more conspicuous during grazing and, therefore, being more prone to predation (i.e. copepods^{14,88,89}). Arias *et al.*⁸⁵ also found that diel rhythms of feeding were modulated by hunger and satiation; only satiated protozoans showed full amplitude diel feeding rhythms. A similar response to food availability was also observed in copepods¹⁴. However, contrary to expectations, diel feeding rhythms in upwelling areas were fuzzy compared to areas with low food

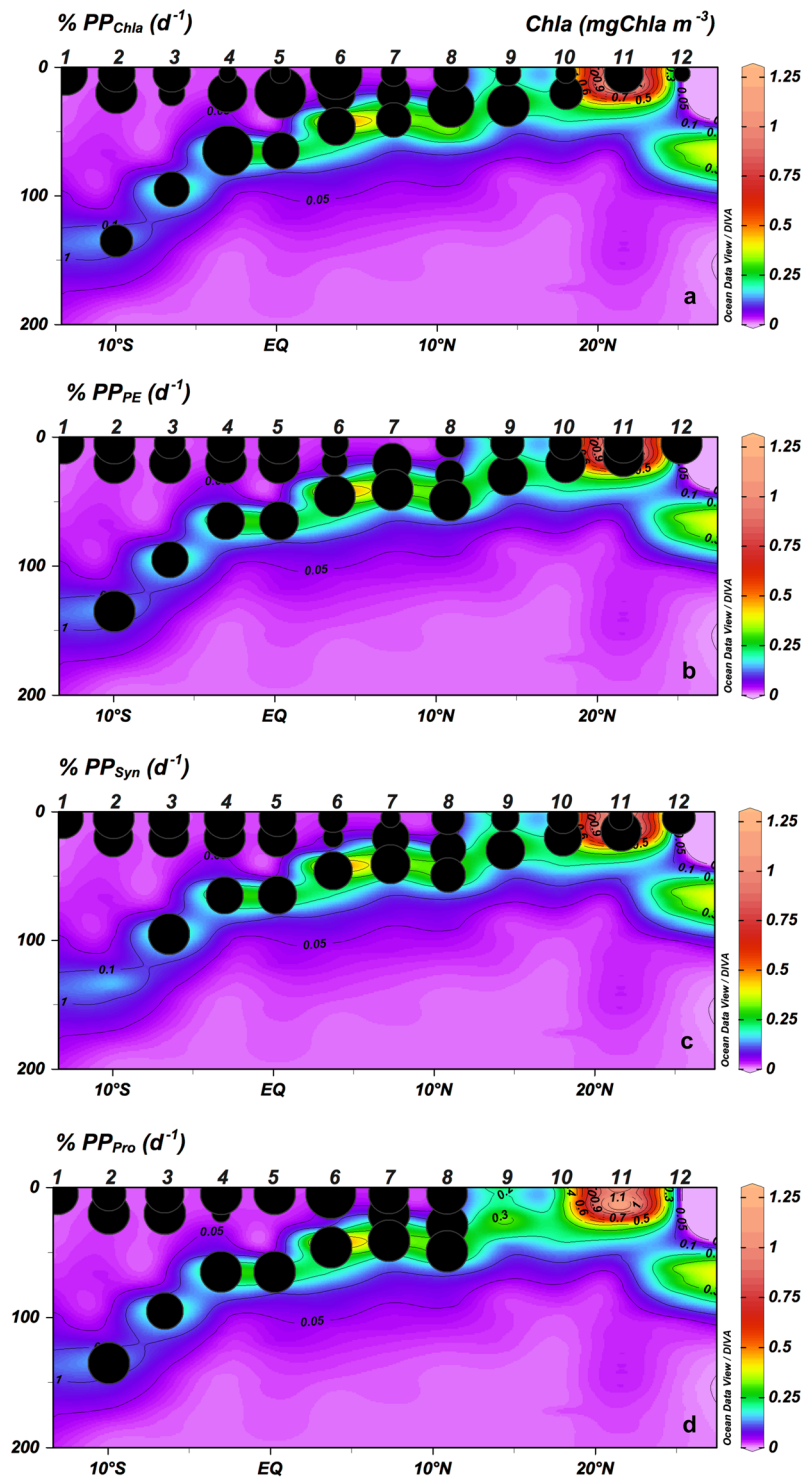


Figure 9. Vertical section (0–200 m) of Chlorophyll *a* (mgChla m^{-3}) and microzooplankton grazing on potential phytoplankton production (% PP) for (a) Chlorophyll *a* (% PP_{Chla}), (b) picoeukaryotes (% PP_{PE}), (c) *Synechococcus* (% PP_{Syn}) and (d) *Prochlorococcus* (% PP_{Pro}).

availability. We propose two alternative hypotheses to explain this. On one hand, species adapted to low food environments may have satiation thresholds at lower concentrations than those adapted to richer environments. On the other hand, given the specificity of the diel feeding response^{84,85}, it is possible to explain the variations in diel feeding behaviour by changes in the composition of the μZ community. Backing up this hypothesis, we found oligotrophic areas being dominated by *Din* (usually showing more evident diel grazing rhythms than *Cil*⁸⁴), whereas the μZ of more productive waters, mostly dominated by *Cil*, seems to be highly species-specific in their diel behaviours⁸⁴.

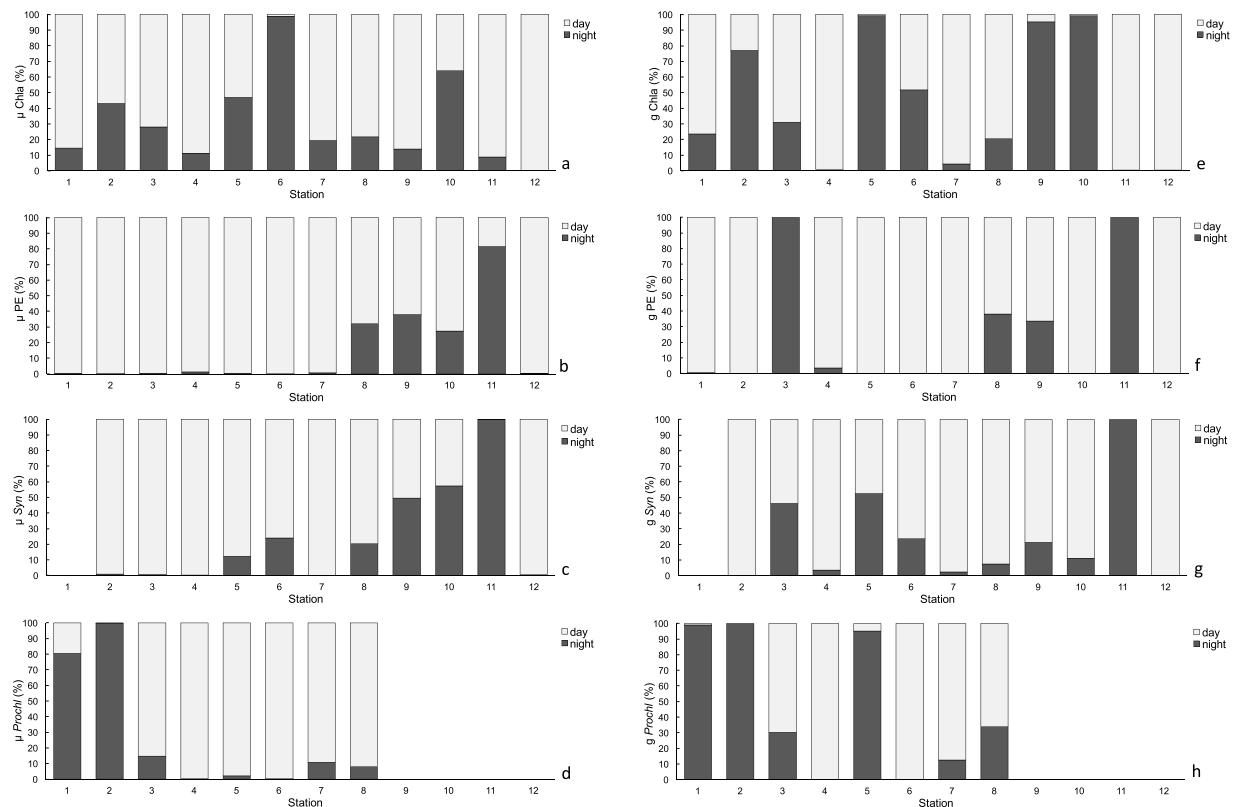


Figure 10. Proportion of phytoplankton potential growth (μ) rates for (a) Chlorophyll *a* (Chla), (b) picoeukaryotes (PE), (c) *Synechococcus* (Syn) and (d) *Prochlorococcus* (Proch) and microzooplankton grazing (g) rates for (e) Chlorophyll *a* (Chla), (f) picoeukaryotes (PE), (g) *Synechococcus* (Syn) and (h) *Prochlorococcus* (Proch) during day (light bars) and night (dark bars) hours at each station.

Summary. In summary, across the tropical and subtropical Atlantic Ocean, we found a close relationship between physico-chemical variables and the distribution of planktonic organisms. These changes in distribution and species composition in turn drive the trophic relationships within plankton, consolidating the paradigms of a more complex and efficient nutrient recycling microbial food web in the oligotrophic ocean compared with a “classic” and shorter one in more productive areas.

Material and Methods

Sampling and hydrographic measurements. Sampling took place from 5th to 29th April, 2015 on board the R.V. *Hespérides* from Salvador da Bahia (Brazil) to Canary Islands (Spain). Twelve stations were sampled between 13°S–25°N (Fig. 11, Table 4), and at each station two casts were conducted using a General Oceanics rosette equipped with 24 L PVC Niskin bottles and Seabird 911-plus CTD equipped with a Seapoint Chlorophyll Fluorometer and a Seabird-43 Dissolved Oxygen Sensor. The first cast was carried out down to 3500 m depth during night, and the second cast was carried out from the surface to 200 m depth during daylight hours. Vertical distribution of the photosynthetically active irradiance (PAR, 400–700 nm) was measured using a radiometer Biospherical/Licor installed in the rosette sampler. Water samples to calibrate dissolved oxygen sensor were collected with Niskin bottles along all the water column.

Nutrients and oxygen. Inorganic nutrients were sampled from hydrographic bottles with polyethylene tubes and stored frozen (−20 °C) until their analysis in the laboratory. Samples were analysed with a QuAatro 39-SEAL Analytical AutoAnalyzer following the protocol by Armstrong *et al.*¹⁶. On board oxygen calibration was carried out with the potentiometric end-point Winkler method⁹⁰.

Chlorophyll *a* and picoplankton. Chla samples were taken at 5 levels from the surface to 200 m depth in order to calibrate the fluorescence sensor installed in the rosette. Samples of 500 mL were collected from the Niskin bottles, filtered through 25 mm Whatman GF/F filters and stored frozen until their analysis. In the laboratory, pigments were extracted in cold acetone (90%) for 24 h and analysed using an AU TurnerDesigns bench fluorometer previously calibrated with pure Chla (Sigma Aldrich) according to Yentsch & Menzel⁹¹ and acidified following Welschmeyer⁹². Chla concentration was converted to carbon assuming a C:Chl of 50⁹³ since conversion ratio for the studied area ranged from 30 to 80, being more quoted around 50.

Station	Time	Growth (h^{-1})				Grazing (h^{-1})			
		μ_{Chla}	μ_{PE}	μ_{Syn}	μ_{Proch}	g_{Chla}	g_{PE}	g_{Syn}	g_{Proch}
1	Day	n.s	0.037 ± 0.004		0.002 ± 0.002	n.s	0.23 ± 0.001		0.000 ± 0.001
	Night	n.s	0.001		0.010 ± 0.011	n.s	0.001		0.015 ± 0.002
2	Day	0.006 ± 0.005	0.049 ± 0.021	0.010 ± 0.001	0.001	0.002 ± 0.002	0.074 ± 0.007	0.033 ± 0.004	0.000 ± 0.014
	Night	0.004 ± 0.001	0.001	0.001	0.024 ± 0.011	0.006 ± 0.002	0.001	0.001	0.023 ± 0.006
3	Day	0.029 ± 0.000	0.028 ± 0.005	0.017 ± 0.001	0.059 ± 0.003	0.015 ± 0.001	0.001	0.006 ± 0.002	0.037 ± 0.007
	Night	0.011 ± 0.000	0.001	0.001	0.010 ± 0.002	0.007 ± 0.000	0.005 ± 0.004	0.005 ± 0.001	0.016 ± 0.002
4	Day	0.030 ± 0.003	0.052 ± 0.014	0.031 ± 0.001	0.022 ± 0.006	0.013 ± 0.018	0.043 ± 0.004	0.019 ± 0.003	0.016 ± 0.003
	Night	0.004 ± 0.001	0.001	0.001	0.001	0	0.002 ± 0.001	0.001 ± 0.001	0.001
5	Day	0.010 ± 0.003	0.029 ± 0.007	0.025 ± 0.009	0.005 ± 0.001	0	0.026 ± 0.001	0.008 ± 0.004	0.000 ± 0.002
	Night	0.009 ± 0.005	0.001	0.003 ± 0.001	0.001	0.014 ± 0.004	0.001	0.009 ± 0.001	0.004 ± 0.002
6	Day	0.001	0.056 ± 0.001	0.032 ± 0.007	0.038 ± 0.004	0.003 ± 0.003	0.087 ± 0.001	0.017 ± 0.001	0.030 ± 0.003
	Night	0.010 ± 0.000	0.001	0.010 ± 0.000	0.001	0.004 ± 0.002	0.001	0.005 ± 0.004	0.001
7	Day	0.027 ± 0.001	0.017 ± 0.008	0.076 ± 0.003	0.026 ± 0.005	0.013 ± 0.002	0.013 ± 0.001	0.014 ± 0.003	0.024 ± 0.005
	Night	0.007 ± 0.002	0.001	0.001	0.003 ± 0.001	0.001 ± 0.002	0.001	0.000 ± 0.004	0.003 ± 0.003
8	Day	0.028 ± 0.004	0.019 ± 0.007	0.053 ± 0.008	0.021 ± 0.007	0.021 ± 0.003	0.008 ± 0.002	0.044 ± 0.002	0.012 ± 0.000
	Night	0.008 ± 0.001	0.009 ± 0.004	0.014 ± 0.002	0.002 ± 0.003	0.005 ± 0.001	0.005 ± 0.001	0.004 ± 0.002	0.006 ± 0.000
9	Day	0.026 ± 0.005	0.034 ± 0.002	0.034 ± 0.007		0	0.025 ± 0.001	0.030 ± 0.001	
	Night	0.004 ± 0.000	0.021 ± 0.002	0.034 ± 0.003		0.002 ± 0.000	0.013 ± 0.001	0.008 ± 0.001	
10	Day	0.005 ± 0.001	0.028 ± 0.004	0.016 ± 0.005		0	0.046 ± 0.001	0.027 ± 0.003	
	Night	0.009 ± 0.001	0.011 ± 0.002	0.021 ± 0.001		0.015 ± 0.002	0.001	0.003 ± 0.002	
11	Day	0.021 ± 0.001	0.003 ± 0.002	0.001		0.019 ± 0.001	0.001	0.001	
	Night	0.002 ± 0.000	0.012 ± 0.003	0.026 ± 0.001		0	0.014 ± 0.001	0.015 ± 0.001	
12	Day	0.047 ± 0.004	0.021 ± 0.008	0.017 ± 0.003		0.018 ± 0.002	0.013 ± 0.003	0.019 ± 0.001	
	Night	0.0001	0.001	0.001		0	0.001	0.001	

Table 3. Phytoplankton growth (μ) and microzooplankton grazing (g) rates (d^{-1}) for total chlorophyll a (Chla), picoeukaryotes (PE), *Synechococcus* (Syn) and *Prochlorococcus* (Proch) from superficial waters dilution experiments (5 m) during daylight and night hours. Negative growth and grazing rates were converted to 0.001 and 0 respectively. Note *Proch* were not present from station 9 to 12. Values (mean \pm SE).

In order to better define the upwelling stations, PP data were obtained from the Ocean Productivity website using the VGPM model following Behrenfeld and Falkowski⁹⁴ (<http://www.science.oregonstate.edu/ocean.productivity/index.php>).

Picoplankton samples were taken from the initial conditions of the 100% whole seawater (WSW) treatments of grazing experiments (see “Microzooplankton grazing experiments”). PE, Syn and *Proch* were counted by flow cytometry using FACScalibur cytometer (Becton and Dickinson)⁹⁵. Abundance was converted to biomass using the carbon conversion factor of 1500 fgC cell⁻¹ for PE⁹⁶, 29 fgC cell⁻¹ for *Proch* and 100 fgC cell⁻¹ for Syn⁹⁷.

Micro- and mesozooplankton stock measurements. Microplankton samples were collected directly from the Niskin bottle during the daylight cast at 5 m depth (surface), mixed layer (20–30 m) and Chla maximum depth (Table 4). Samples of 500 mL were preserved in alkaline Lugol's solution until their analysis in the laboratory. An aliquot of 100 mL of each sample was allowed to settle using sedimentation chambers⁹⁸ and analysed on an inverted Olympus IX83 microscope equipped with a motorized focus drive. The microscope was controlled by CellSens software using the automated image acquisition at 200x magnification. More than 25% of total sample area (minimum of 300 organisms counted) was imaged using the functions of Multiple Image Aligning (MIA) and Z-stack. MIA takes pictures of an area and the Z-stack gets images in the Z plane. Identification and counting of organisms was carried out manually from the digital image. Main microplankton groups were identified: Dia, Din, tintinnids and Cil. Din, considered all as μZ , and Cil were counted as $<20 \mu m$, $20-40 \mu m$ $>40 \mu m$ in order to convert abundance to biomass more accurately. The biovolume of each organism was calculated from its equivalent spherical diameter (ESD) and converted to biomass^{89,99}.

MZ samples were collected during daylight hours at each station with a Multiple Opening and Closing Net and Environmental Sensing System (MOCNESS) equipped with a 200 μm mesh net at 0–50, 50–100 and 100–200 m depth intervals. Oblique trawls were conducted at a towing speed of ca. 3 knots, measuring the volume of water filtered using a calibrated electronic flowmeter. MZ biomass was directly obtained on board through image processing using the software ZooImage 1, version 1.2-1¹⁰⁰ and using a conversion factor from Uye¹⁰¹.

Microzooplankton grazing experiments. To estimate μZ grazing upon phytoplankton, dilution experiments were carried out using the 2-treatments method¹⁰² based on the seawater dilution technique^{103,104}. Briefly, seawater in two treatments consisting in 100 and 5% whole seawater (WSW) was incubated for 24 h to obtain the net growth rate of phytoplankton. The 100% WSW treatment is used to measure the net growth rate of phytoplankton (k), while the intrinsic growth rate (μ) is measured from the 5% WSW treatment. μZ grazing rate (g) was

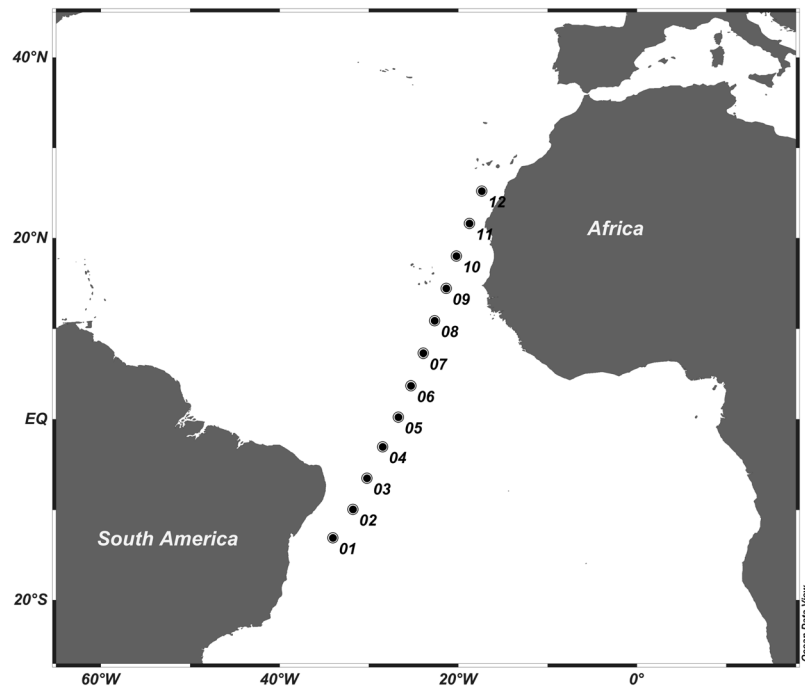


Figure 11. Map of the study area across the Atlantic Ocean.

Station	Latitude	Longitude	Depth (m)	Temperature (° C)	Salinity	Dissolved O ₂ (μmol Kg ⁻¹)
1	-13.12	-34.05	5	28.54	37.02	236.17
2	-9.96	-31.79	5	28.79	36.66	222.73
			20	28.43	36.66	156.31
			135	21.74	36.65	157.71
3	-6.51	-30.22	5	28.74	36.35	184.32
			20	28.6	36.35	155.02
			95	23.95	36.46	177.18
4	-3.03	-28.46	5	29.39	35.75	314.15
			20	28.65	36.01	159.68
			65	22.24	36.20	123.94
5	0.25	-26.70	5	28.45	35.78	255.37
			20	28.10	35.96	159.48
			65	22.64	36.42	146.71
6	3.73	-25.32	5	28.14	35.89	252.51
			20	27.86	35.91	158.43
			46	18.65	35.78	112.55
7	7.30	-23.93	5	25.73	35.73	199.51
			20	25.04	35.75	166.03
			41	21.26	36.00	145.73
8	10.87	-22.65	5	24.13	35.73	210.41
			29	23.72	35.76	169.47
			49	21.18	35.72	160.18
9	14.44	-21.36	5	22.09	35.90	173.51
			30	21.92	35.90	172.38
10	18.04	-20.22	5	20.10	36.00	177.00
			20	20.07	35.99	173.88
11	21.63	-18.76	5	17.98	35.91	163.43
			15	17.69	35.90	205.50
12	25.24	-17.38	5	19.32	36.64	181.81

Table 4. Location of the studied stations and initial conditions for microzooplankton grazing experiments.

Station	Date	Sampling time	Sampling hour (UTC)
1	05/04/2015	T = 0	16:06
		T = 12	4:05
		T = 24	16:08
2	07/04/2015	T = 0	19:35
		T = 12	8:37
		T = 24	19:33
3	09/04/2015	T = 0	18:39
		T = 12	7:42
		T = 24	18:45
4	11/04/2015	T = 0	19:34
		T = 12	7:40
		T = 24	19:39
5	13/04/2015	T = 0	19:30
		T = 12	07:40
		T = 24	19:35
6	15/04/2019	T = 0	19:30
		T = 12	7:37
		T = 24	19:40
7	17/04/2015	T = 0	19:20
		T = 12	7:25
		T = 24	19:20
8	19/04/2015	T = 0	18:56
		T = 12	7:08
		T = 24	19:00
9	21/04/2015	T = 0	19:35
		T = 12	7:40
		T = 24	19:43
10	23/04/2015	T = 0	21:04
		T = 12	8:55
		T = 24	21:11
11	25/04/2015	T = 0	19:35
		T = 12	7:40
		T = 24	19:46
12	27/04/2015	T = 0	19:37
		T = 12	7:44
		T = 24	19:38

Table 5. Location and time sampling during daily phytoplankton growth and mortality experiments at depth of 5 m.

obtained from $g = \mu - k$. Negative values of μ were converted to 0.001 d^{-1} , while negative values of g were converted to 0 d^{-1} ²⁸.

Water for experiments was collected at the surface (5 m depth), mixed layer (20 m) and at the chlorophyll maximum (CM) during the daylight cast (Table 4). Vertical PAR distribution was measured prior to incubation and light profiles were simulated on board incubator using a set of neutral density and blue plastic filters²⁵. Temperature was controlled using a series of Titan 2000 coolers. Each experiment was carried out in triplicate using 3.4 L Tedlar[®] bags during 24 h. The 100% WSW was gently screened with a 200 μm mesh net to avoid MZ, while the filtered seawater was gravity-filtered through 0.2 μm Whatman[®] Polycap filter. Experiments were run with added nutrients at saturating concentrations in all stations. Nutrient concentration were obtained from Chla concentration observed by Marañón *et al.*²⁵ and converted first to C^{93} and then to N and P using the Redfield ratio (final nutrient concentrations were: 2–6 μM of NH_4Cl and 0.1–0.5 μM of Na_2HPO_4). Chla and picoplankton were sampled at $t = 0$ h (initial conditions) and $t = 24$ h from each treatment (see methods of analysis above).

The impact of μZ grazing on phytoplankton production was estimated using the ratio $g:\mu$ for Chla, PE, *Syn* and *Proch*²⁸. It should be noted that we added nutrients to the bottles in order to warrant a critical assumption of the dilution method (phytoplankton growth rates should be independent from the dilution level¹⁰³). Thus, we obtained potential growth rates of phytoplankton.

Diel phytoplankton growth and mortality. In order to study the daily phytoplankton growth and mortality, dilution grazing experiments were carried out using surface waters (5 m depth). Incubations lasted for 24 h, but there was an intermediate sampling at $t = 12$ h (early in the morning); after 24 h, (near dusk) final samples were taken and the experiments terminated (Table 5). This depth was selected because the signature of the diel

rhythm should be stronger at more illuminated layers, and organisms at the surface are less photosensitive than those inhabiting deeper layers. In this sense, natural variations in light such as clouds or waves, as well as manipulation have a lower impact on surface organisms than most light sensitive organisms.

Statistical analysis. Principal component analysis (PCA) was used to reduce the dimensionality of physical and biological variables (R Project software). We used the cumulative proportion and the histogram of variances by components to determine the total amount of variance explained by the main components, using those where the variance was >60% of. Then, we interpreted each main component in terms of the original variables, examining both graph of influences and, the magnitude and direction of original coefficients. During PCA analysis, no outlier has been eliminated since the cumulative proportion and the proportion of the variance could explain >60% of the variability. Generalized additive modelling (GAM) was used to explore the dependence between biological and physical parameters (R Project software), using factors from PCA (see Supplementary Equations and Supplementary Fig. 1). Kendall Rank correlation coefficients were used to study the relationships between biomass, mortality rates, and environmental variables (Supplementary Table 4). Kendall Rank is preferable to Spearman test because of its robustness and efficiency in the study of populations with scarcely or tied data. For statistical comparisons, a t-test was used for data with a normal distribution and a Wilcoxon-Mann-Whitney for data with no normal distribution. To study the normality of data, a Shapiro-Wilk test was performed. We carried out the Wilcoxon test to investigate differences between growth and mortality during the day and night (Statistica software). The limit between oligotrophic and productive areas was established at 0.5 mgChla m⁻³ in surface and mixed layer¹⁰⁵.

References

- Del Giorgio, P. A. & Williams, P. J. leB. *Respiration in aquatic ecosystems*. (Oxford University Press, 2005).
- Schmoker, C., Hernández-León, S. & Calbet, A. Microzooplankton grazing in the oceans: impacts, data variability, knowledge gaps and future directions. *J. Plankton Res.* **35**, 691–706 (2013).
- Calbet, A., Alcaraz, M., Saiz, E., Estrada, M. & Trepast, I. Planktonic herbivorous food webs in the Catalan Sea (NW Mediterranean): temporal variability and comparison of indices of phyto-zooplankton coupling based on state variables and rate processes. *Journal of Plankton Research* **18** (1996).
- Falkowski, P. G., Barber, R. T. & Smetacek, V. Biogeochemical Controls and Feedbacks on Ocean Primary Production. *Science* **281**(5374), 200–7 (1998).
- Aebischer, N. J., Coulson, J. C. & Colebrook, J. M. Parallel long-term trends across four marine trophic levels and weather. *Nature* **347**, 753–755 (1990).
- Irigoiien, X., Huisman, J. & Harris, R. P. Erratum: Global biodiversity patterns of marine phytoplankton and zooplankton. *Nature* **429**, 863–867 (2004).
- Shurin, J. B. *et al.* A cross-ecosystem comparison of the strength of trophic cascades. *5*(6), 785–791 (2001).
- Polisi, G. A. & Strong, D. R. The American Naturalist. **147** (1996).
- Weitz, J. S. *et al.* A multitrophic model to quantify the effects of marine viruses on microbial food webs and ecosystem processes. *ISME J.* **9**, 1352–64 (2015).
- Legendre, L. & Rassoulzadegan, F. Plankton and nutrient dynamics in marine waters. *Ophelia* **41**, 153–172 (1995).
- Schmoker, C. *et al.* Effects of eutrophication on the planktonic food web dynamics of marine coastal ecosystems: The case study of two tropical inlets. *Mar. Environ. Res.* **119**, 176–188 (2016).
- Christaki, U. *et al.* Microbial food web dynamics during spring phytoplankton blooms in the naturally iron-fertilized Kerguelen area (Southern Ocean). *Biogeosciences* **11**, 6739–6753 (2014).
- Billen, G., Servais, P. & Becquevort, S. Dynamics of bacterioplankton in oligotrophic and eutrophic aquatic environments: bottom-up or top-down control? *Hydrobiologia* **207**, 37–42 (1990).
- Calbet, A. & Landry, M. R. Mesozooplankton influences on the microbial food web: Direct and indirect trophic interactions in the oligotrophic open ocean. *Limnol. Oceanogr.* **44** (1999).
- Sommer, U., Stibor, H., Katschik, A., Sommer, F. & Hansen, T. Pelagic food web configurations at different levels of nutrient richness and their implications for the ratio fish production:primary production. In Sustainable Increase of Marine Harvesting: Fundamental Mechanisms and New Concepts 11–20, (Springer Netherlands, 2002), https://doi.org/10.1007/978-94-017-3190-4_2.
- Armstrong, F. A. J., Stearns, C. R. & Strickland, J. D. H. The measurement of upwelling and subsequent biological process by means of the Technicon Autoanalyzer[®] and associated equipment. *Deep Sea Res. Oceanogr. Abstr.* **14**, 381–389 (1967).
- Décima, M., Landry, M. R., Stukel, M. R., Lopez-Lopez, L. & Krause, J. W. Mesozooplankton biomass and grazing in the Costa Rica Dome: amplifying variability through the plankton food web. *J. Plankton Res.* **38**, 317–330 (2016).
- Polovina, J. J., Howell, E. A. & Abecassis, M. Ocean's least productive waters are expanding. *Geophys. Res. Lett.* **35**, L03618 (2008).
- Assmy, P. *et al.* Response of the protozooplankton assemblage during the European Iron Fertilization Experiment (EIFEX) in the Antarctic circumpolar current. *J. Plankton Res.* **36**, 1175–1189 (2014).
- Sherr, E. B. & Sherr, B. F. Bacterivory and Herbivory: Key Roles of Phagotrophic Protists in Pelagic Food Webs. *Source: Microbial Ecology* **28** (1994).
- Boëchat, I. G., Weithoff, G., Krüger, A., Gücker, B. & Adrian, R. A biochemical explanation for the success of mixotrophy in the flagellate *Ochromonas* sp.
- Jones, R. I. Jones 2000 - Mixotrophy in planktonic protists.pdf. 219–226 (2000).
- Laws, E. A., Ditullio, G. R. & Redalje, D. G. High phytoplankton growth and production rates in the North Pacific subtropical gyre 1 T2. *Limnol. Oceanogr.* **32** (1987).
- Goericke, R. & Welschmeyer, N. A. Response of Sargasso Sea phytoplankton biomass, growth rates and primary production to seasonally varying physical forcing. *J. Plankton Res.* **20**, 2223–2249 (1998).
- Marañón, E., Holligan, P. M., Varela, M., Mouriño, B. & Bale, A. J. Basin-scale variability of phytoplankton biomass, production and growth in the Atlantic Ocean. *Deep. Res. Part I Oceanogr. Res. Pap.* **47**, 825–857 (2000).
- Quevedo, M. & Anadón, R. Protist control of phytoplankton growth in the subtropical north-east Atlantic. *Mar. Ecol. Prog. Ser.*, <https://doi.org/10.3354/meps221029> (2001).
- Marañón, E. Phytoplankton growth rates in the Atlantic subtropical gyres. *Limnol. Oceanogr.* **50** (2005).
- Calbet, A. & Landry, M. R. Phytoplankton growth, microzooplankton grazing, and carbon cycling in marine systems. *Limnol. Oceanogr.* **49**, 51–57 (2004).
- Calbet, A. The trophic roles of microzooplankton in marine systems. *ICES J. Mar. Sci.* **65**, 325–331 (2008).
- Albert, C. & Michael, R. Phytoplankton growth, microzooplankton grazing, and carbon cycling in marine systems. *Limnol. Oceanogr.* **49**, 51–57 (2004).

31. Saiz, E. & Calbet, A. Copepod feeding in the ocean: scaling patterns, composition of their diet and the bias of estimates due to microzooplankton grazing during incubations. *Hydrobiologia* **666**, 181–196 (2011).
32. Reid, J. L. Evidence of a South Equatorial Countercurrent in the Pacific Ocean. *Nature* **184**, 209–210 (1959).
33. Hartmann, M. *et al.* Comparison of phosphate uptake rates by the smallest plastidic and aplastidic protists in the North Atlantic subtropical gyre. *FEMS Microbiol. Ecol.* **78**, 327–335 (2011).
34. Chisholm, S. W. Phytoplankton Size. In *Primary Productivity and Biogeochemical Cycles in the Sea 213–237*, (Springer US, 1992), https://doi.org/10.1007/978-1-4899-0762-2_12.
35. Marie, D., Partensky, F., Jacquet, S. & Vault, D. Enumeration and Cell Cycle Analysis of Natural Populations of Marine Picoplankton by Flow Cytometry Using the Nucleic Acid Stain SYBR Green I. *Applied and Environmental Microbiology* **63** (1997).
36. Irwin, A. J., Finkel, Z. V., Schofield, O. M. E. & Falkowski, P. G. Scaling-up from nutrient physiology to the size-structure of phytoplankton communities. *J. Plankton Res.* **28**, 459–471 (2006).
37. Veldhuis, M. J. W., Timmermans, K. R., Croot, P. & van der Wagt, B. Picophytoplankton; a comparative study of their biochemical composition and photosynthetic properties. *J. Sea Res.* **53**, 7–24 (2005).
38. DuRand, M. D., Olson, R. J. & Chisholm, S. W. Phytoplankton population dynamics at the Bermuda Atlantic Time-series station in the Sargasso Sea. *Deep Sea Res. Part II Top. Stud. Oceanogr.* **48**, 1983–2003 (2001).
39. Moore, C. M. *et al.* Relative influence of nitrogen and phosphorous availability on phytoplankton physiology and productivity in the oligotrophic sub-tropical North Atlantic Ocean. *Limnology and Oceanography* **53**(1), 291–305 (2008).
40. Moore, J. K., Doney, S. C., Glover, D. M. & Fung, I. Y. Iron cycling and nutrient-limitation patterns in surface waters of the World Ocean. *Deep Sea Res. Part II Top. Stud. Oceanogr.* **49**, 463–507 (2001).
41. Partensky, F., Blanchot, J. & Vault, D. Differential distribution and ecology of Prochlorococcus and Synechococcus in oceanic waters: a review (1999).
42. Martiny, J. B. H. *et al.* Microbial biogeography: putting microorganisms on the map. *Nat. Rev. Microbiol.* **4**, 102–112 (2006).
43. Zubkov, M. V. *et al.* Microbial control of phosphate in the nutrient-depleted North Atlantic subtropical gyre, <https://doi.org/10.1111/j.1462-2920.2007.01324.x> (2007).
44. Tarran, G. A., Heywood, J. L. & Zubkov, M. V. Latitudinal changes in the standing stocks of nano- and picoeukaryotic phytoplankton in the Atlantic Ocean. *Deep Sea Res. Part II Top. Stud. Oceanogr.* **53**, 1516–1529 (2006).
45. Marañón, E., Holligan, P. M., Varela, M., Mouriño, B. & Bale, A. J. Basin-scale variability of phytoplankton biomass, production and growth in the Atlantic Ocean. *Deep Sea Res. Part I Oceanogr. Res. Pap.* **47**, 825–857 (2000).
46. Moore, C. M. *et al.* Processes and patterns of oceanic nutrient limitation. *Nature geoscience* **6**(9), 701 (2013).
47. Daims, H., Lückner, S. & Wagner, M. A New Perspective on Microbes Formerly Known as Nitrite-Oxidizing Bacteria. *Trends Microbiol.* **24**, 699–712 (2016).
48. Cloern, J. Our evolving conceptual model of the coastal eutrophication problem. *Mar. Ecol. Prog. Ser.* **210**, 223–253 (2001).
49. Burkepille, D. E. & Hay, M. E. Herbivore vs. Nutrient Control of Marine Primary Producers: Context-Dependent Effects. *Ecology* **87**, 3128–3139 (2006).
50. Pascal, P.-Y. & Fleeger, J. W. Diverse Dietary Responses by Saltmarsh Consumers to Chronic Nutrient Enrichment. *Estuaries and Coasts* **36**, 1115–1124 (2013).
51. Steffox-Widdicombe, C. E., Edwards, E. S., Burkill, P. H. & Sleigh, M. A. Microzooplankton grazing activity in the temperate and sub-tropical NE Atlantic: Summer 1996. *Mar. Ecol. Prog. Ser.* <https://doi.org/10.3354/meps208001> (2000).
52. Karayanni, H. *et al.* Influence of ciliated protozoa and heterotrophic nanoflagellates on the fate of primary production in the northeast Atlantic Ocean. *J. Geophys. Res.* **110**, C07S15 (2005).
53. Unrein, F., Massana, R., Alonso-Sáez, L. & Gasol, J. M. Unrein, Fernando, Ramon Massana, Laura Alonso-Sáez, and Josep M. Gasol. Significant year-round effect of small mixotrophic flagellates on bacterioplankton in an oligotrophic coastal system. *Limnol. Oceanogr.* **52**(1), 456–469 (2007).
54. Hartmann, M., Zubkov, M. V., Scanlan, D. J. & Lepère, C. *In situ* interactions between photosynthetic picoeukaryotes and bacterioplankton in the Atlantic Ocean: evidence for mixotrophy. *Environ. Microbiol. Rep.* **5**, 835–840 (2013).
55. Fenichel, T. Ecological Physiology: Feeding. in 32–52 (Springer, Berlin, Heidelberg 1987), https://doi.org/10.1007/978-3-662-25981-8_3.
56. Sherr, E. & Sherr, B. Role of microbes in pelagic food webs: A revised concept. *Limnol. Oceanogr.* **33**, 1225–1227 (1988).
57. Christaki, U., Jacquet, S., Dolan, J. R., Vault, D. & Rassoulzadegan, F. Growth and grazing on Prochlorococcus and Synechococcus by two marine ciliates. *Limnol. Oceanogr.* **44** (1999).
58. Huntley, M., Sykes, P., Rohan, S. & Marin, V. Chemically-mediated rejection of dinoflagellate prey by the copepods *Calanus pacificus* and *Paracalanus parvus*: mechanism, occurrence and significance. *Mar. Ecol. Prog. Ser.* **28**(10) (1986).
59. Löder, M. G. J., Meunier, C., Wiltshire, K. H., Boersma, M. & Aberle, N. The role of ciliates, heterotrophic dinoflagellates and copepods in structuring spring plankton communities at Helgoland Roads, North Sea. *Mar. Biol.* **158**, 1551–1580 (2011).
60. Armengol, L., Franchy, G., Ojeda, A., Santana-del Pino, Á. & Hernández-León, S. Effects of copepods on natural microplankton communities: do they exert top-down control? *Mar. Biol.* **164**, 136 (2017).
61. Mallin, M. A. Phytoplankton Ecology of North Carolina Estuaries. **17** (1994).
62. Vargas, C. A. *et al.* The relative importance of microbial and classical food webs in a highly productive coastal upwelling area. *Limnol. Oceanogr.* **52**(4), 1495–1510 (2007).
63. Ward, B. A. & Follows, M. J. Marine mixotrophy increases trophic transfer efficiency, mean organism size, and vertical carbon flux. *Proc. Natl. Acad. Sci. USA* **113**, 2958–63 (2016).
64. Azam, F. *et al.* The Ecological Role of Water-Column Microbes in the Sea. *Marine Ecology Progress Series* **10**, 257–263 (1983).
65. Azam, F. OCEANOGRAPHY: Microbial Control of Oceanic Carbon Flux: The Plot Thickens. *Science (80-)*. **280**, 694–696 (1998).
66. Pomeroy, L. R., leB. WILLIAMS, P. J., Azam, F. & Hobbie, J. E. The microbial loop. *Oceanography* **20**(2), 28–33 (2007).
67. Landry, M. R., Ohman, M. D., Goericke, R., Stukel, M. R. & Tsyrlkevich, K. Lagrangian studies of phytoplankton growth and grazing relationships in a coastal upwelling ecosystem off Southern California. *Prog. Oceanogr.* **83**, 208–216 (2009).
68. Cullen, J. J. The Deep Chlorophyll Maximum: Comparing Vertical Profiles of Chlorophyll a. *Can. J. Fish. Aquat. Sci.* **39**, 791–803 (1982).
69. Goericke, R. *Pigments as ecological tracers for the study of the abundance and growth of marine phytoplankton* Ph.D. (Harvard University, 1990).
70. Worden, A. Z. & Binder, B. J. Application of dilution experiments for measuring growth and mortality rates among Prochlorococcus and Synechococcus populations in oligotrophic environments. *Aquat. Microb. Ecol.* <https://doi.org/10.3354/ame030159> (2003).
71. Siegel, D. A., Dickey, T. D., Washburn, L., Hamilton, M. K. & Mitchell, B. G. Optical determination of particulate abundance and production variations in the oligotrophic ocean. *Deep-Sea Research* **36** (1989).
72. Gardner, W. D., Chung, S. P., Richardson, M. J. & Walsh, I. D. The oceanic mixed-layer pump. *Deep Sea Res. Part II Top. Stud. Oceanogr.* **42**, 757–775 (1995).
73. Claustre, H. *et al.* Diel variations in Prochlorococcus optical properties. *Limnol. Oceanogr.* **47** (2002).
74. MacIntyre, H. L., Kana, T. M. & Geider, R. J. The effect of water motion on short-term rates of photosynthesis by marine phytoplankton. *Trends Plant Sci.* **5**, 12–17 (2000).
75. Edmunds, K. A. L. N. Jr. Clocked cell cycle clocks. *Science (80-)*. **211**, 1002–1013 (1981).

76. Sweeney, B. M. & Borgese, M. B. A Circadian Rhythm in Cell Division in a Prokaryote, the Cyanobacterium *Synechococcus* Wh78031. *J. Phycol.* **25**, 183–186 (1989).
77. Jacquet, S., Partensky, F., Lennon, J.-F. & Vaulot, D. Diel Patterns of Growth and Division in Marine Picoplankton in Culture 1. *J. Phycol.* **37**, (2001).
78. Ribalet, F. *et al.* Light-driven synchrony of *Prochlorococcus* growth and mortality in the subtropical Pacific gyre. *Proc. Natl. Acad. Sci.* **112**, 8008–8012 (2015).
79. Diamond, S., Jun, D., Rubin, B. E. & Golden, S. S. The circadian oscillator in *Synechococcus elongatus* controls metabolite partitioning during diurnal growth, <https://doi.org/10.1073/pnas.1504576112>.
80. Dimier, C., Brunet, C., Geider, R. & Raven, J. Growth and photoregulation dynamics of the picoeukaryote *Pelagomonas calceolata* in fluctuating light. *Limnology and Oceanography* **54**(3), 823–836 (2009).
81. Skovgaard, A. Role of chloroplast retention in a marine dinoflagellate. **15** (1998).
82. Strom, S. Light-aided digestion, grazing and growth in herbivorous protists. *Aquat. Microb. Ecol.* **23**, 253–261 (2001).
83. Jakobsen, H. H. & Strom, S. L. Circadian protist plankton cycles in growth and feeding rates of heterotrophic. *Limnology* **49**, 1915–1922 (2008).
84. Jakobsen, H. H. & Strom, S. L. Circadian cycles in growth and feeding rates of heterotrophic protist plankton. *Limnol. Oceanogr.* **49**, (2004).
85. Arias, A., Saiz, E. & Calbet, A. Diel feeding rhythms in marine microzooplankton: effects of prey concentration, prey condition, and grazer nutritional history. *Mar. Biol.* **164**, 205 (2017).
86. Ng, W. H. A. & Liu, H. Diel periodicity of grazing by heterotrophic nanoflagellates influenced by prey cell properties and intrinsic grazing rhythm. *J. Plankton Res.* **38**, 636–651 (2016).
87. Ng, W. H. A., Liu, H. & Zhang, S. Diel variation of grazing of the dinoflagellate *Lepidodinium* sp. and ciliate *Euplotes* sp. on algal prey: the effect of prey cell properties. *J. Plankton Res.* **39**, 450–462 (2017).
88. Calbet, A., Calbet, A. & Saiz, E. The Ciliate-Copepod Link in Marine Ecosystems The ciliate-copepod link in marine ecosystems. **38**, 157–167 (2015).
89. Montagnes, D. J. S., Berges, J. A., Harrison, P. J. & Taylor, F. J. R. Estimating carbon, nitrogen, protein, and chlorophyll a from volume in marine phytoplankton. *Limnol. Oceanogr.* **39** (1994).
90. Moreno-Ostos, E. Libro blanco de métodos y técnicas de trabajo oceanográfico. *Proceeding of Expedición de Circunnavegación MALASPINA* (2010).
91. Yentsch, C. S. & Menzel, D. W. A method for the determination of phytoplankton chlorophyll and phaeophytin by fluorescence*. (1963).
92. Welschmeyer, N. A. Fluorometric analysis of chlorophyll a in the presence of chlorophyll b and pheopigments. *Limnol. Oceanogr.* **39**, 1985–1992 (1994).
93. Harris, G. P. *Phytoplankton Ecology: Structure, Function and Fluctuation*. xi, 384 pp. Chapman and Hall, 1986. Price £30.00. *J. Mar. Biol. Assoc. United Kingdom* **67**, 235 (1987).
94. Behrenfeld, M. J. & Falkowski, P. G. Photosynthetic rates derived from satellite-based chlorophyll concentration. *Limnol. Oceanogr.* **42**, 1–20 (1997).
95. Gasol, J. M. & Del Giorgio, P. A. Using flow cytometry for counting natural planktonic bacteria and understanding the structure of planktonic bacterial communities. *Sci. Mar.* **64**, 197–224 (2000).
96. Zubkov, M. V., Sleight, M. A., Tarran, G. A., Burkill, P. H. & Leakey, R. J. Picoplanktonic community structure on an Atlantic transect from 50°N to 50°S. *Deep Sea Res. Part I Oceanogr. Res. Pap.* **45**, 1339–1355 (1998).
97. Zubkov, M. V., Sleight, M. A., Burkill, P. H. & Leakey, R. J. G. Picoplankton community structure on the Atlantic Meridional Transect: a comparison between seasons. *Prog. Oceanogr.* **45**, 369–386 (2000).
98. Utermöhl, H. Zur vervollkommnung der quantitativen phytoplankton methodik (1958).
99. Zarauz, L., Irigoien, X. & Fernandes, J. A. Changes in plankton size structure and composition, during the generation of a phytoplankton bloom, in the central Cantabrian sea. *J. Plankton Res.* **31**, 193–207 (2008).
100. Garijo, J. C. & Carlos, J. Zooplankton biomass and metabolism through image analysis systems: from the development and testing of metabolic equations to the assessment of carbon fluxes (2016).
101. Uye, S. Length-weight relationships of important zooplankton from the Inland Sea of Japan. *J. Oceanogr. Soc. Japan* **38**, 149–158 (1982).
102. Strom, S. L. & Fredrickson, K. A. Intense stratification leads to phytoplankton nutrient limitation and reduced microzooplankton grazing in the southeastern Bering Sea. *Deep. Res. Part II Top. Stud. Oceanogr.* **55**, 1761–1774 (2008).
103. Prog, S., Landryl, M. R., Haas2, L. W. & Fagerness, V. L. Marine Ecology-Progress Series Dynamics of microbial plankton communities:*** experiments in Kaneohe Bay, Hawaii. **16** (1984).
104. Landry, M. R. & Hassett, R. P. Marine Biology Estimating the Grazing Impact of Marine Micro-zooplankton*. *Marine Biology* **67** (1982).
105. Grodsky, S. A., Carton, J. A. & McClain, C. R. Variability of upwelling and chlorophyll in the equatorial Atlantic. *Geophys. Res. Lett.* **35**, L03610 (2008).

Acknowledgements

This research was funded by projects Migrants and Active Flux in the Atlantic Ocean (MAFIA, CTM2012-39587-C04-01) to S.H.L. and Daily feeding rhythms in marine microzooplankton (FERMI, CGL2014-59227-R; MINECO/FEDER, UE) to A.C. L.A. was funded with a doctoral fellowship (BES-2013-063148) from the MINECO of Spain. We are grateful to Dr. J.C. Garijo for the mesozooplankton data and Marie Magendie. This article is a publication of the Unidad Océano y Clima of the Universidad de Las Palmas de Gran Canaria R&D&CSIC-associate unit.

Author Contributions

L.A. and S.H.-L. designed the research; A.R.-S. and G.F. performed the research; L.A. analysed the samples; L.A., A.C. and S.H.-L. wrote the paper.

Additional Information

Supplementary information accompanies this paper at <https://doi.org/10.1038/s41598-019-38507-9>.

Competing Interests: The authors declare no competing interests.

Publisher's note: Springer Nature remains neutral with regard to jurisdictional claims in published maps and institutional affiliations.



Open Access This article is licensed under a Creative Commons Attribution 4.0 International License, which permits use, sharing, adaptation, distribution and reproduction in any medium or format, as long as you give appropriate credit to the original author(s) and the source, provide a link to the Creative Commons license, and indicate if changes were made. The images or other third party material in this article are included in the article's Creative Commons license, unless indicated otherwise in a credit line to the material. If material is not included in the article's Creative Commons license and your intended use is not permitted by statutory regulation or exceeds the permitted use, you will need to obtain permission directly from the copyright holder. To view a copy of this license, visit <http://creativecommons.org/licenses/by/4.0/>.

© The Author(s) 2019